Journal of Engineering Mathematics **42:** 91–118, 2002.

On the motion of a spherical bubble deforming near a plane wall

C.W.M. VAN DER GELD
Eindhoven University of Technology, Faculty of Mechanical Engineering, W-hoog 4.130, P.O. Box 513, 5600 MB Eindhoven, The Netherlands (e-mail: c.w.m.v.d.geld@wtb.tue.nl)

Received 13 June 2001; accepted in revised form 4 July 2001

Abstract. Equations of motion are derived for an expanding spherical bubble in potential flow near a plane wall using the Lagrange-Thomson method and an extended Rayleigh dissipation function to account for the drag. This method is shown to yield the same acceleration of the bubble center as that obtained using the Lagally theorem. An extended Rayleigh-Plesset equation is derived to describe deformation in the vicinity of a plane wall, and expressions relating the drag force to the distance from the wall and the bubble growth rate are derived. The solution method for the velocity potential can also be applied to the case of non-spherical deformation.

Key words: bubble dynamics, deformable body, Lagally theorem, drag force, Lagrangian method, Rayleigh dissipation function.

1. Introduction

Bubble detachment from surfaces and subsequent oscillatory motion occur in engineering processes involving phase-change transition. To predict the bubble size and analyze the dynamics of the unsteady motion after detachment, accurate information on the magnitude of the inertial and drag forces exerted on bubbles near a plane wall is required. Even if turbulence and boundary layers on walls are neglected, the engineering prediction of bubble size at detachment is limited by a lack of knowledge. Usually expressions for forces exerted on solitary bubbles in an infinite liquid are gathered in a force balance, and empirical constants are introduced to fit experimental results for bubbles detaching from a plane wall [1, 2]. Several authors presented numerical predictions (see Yuan and Prosperetti [3] and Pelekasis and Tsamopoulos [4]), but these predictions do not yield expressions for the forces on the bubble as a whole that can be used for engineering prediction. Existing analytical solutions do yield general expressions, but are only available for bubbles far away from a wall, *i.e.*, for an infinite liquid.

Solutions of the Rayleigh–Plesset (R.P.) equation for a radially expanding spherical bubble in an unbounded incompressible fluid have been used to generate simple expressions for the force and bubble growth rate. The R.P. equation is usually derived by integration of the full radial Navier–Stokes equation [5]. Analytical solutions of the R.P. equation proved useful for the undertanding and engineering prediction of cavitation and boiling phenomena [6] in the absence of walls.

A mirror bubble can be introduced to account for the presence of a wall, yielding a system of two equally sized bubbles pulsating in phase. The study of the hydrodynamic interaction of two *linearly* oscillating bubbles has a long history dating back to Bjerknes. This linear theory is well understood [7–9]. *Nonlinear* oscillions have been studied by several authors in

the last decade mainly by numerical methods, see, *e.g.*, [4]. Oguz *et al.* [10] derived a set of generalized impulse and virial theorems and found some approximate solutions.

A powerful formalism to generate analytical results is provided by the Lagrange-Hamilton theory. Constants of motion are readily generated, and the relation between symmetries and conservation laws are unraveled [11]. The formalism allows for non-uniform flow fields [12] and can accommodate concepts of statistical mechanics [13]. The Lagrangian approach was first applied to the motion of a finite number of solids in a frictionless fluid by Thomson and Tait [14, Chapter 6], and Kirchhoff [14, Chapter 6]. Approximate solutions for the case of a single solid sphere in the presence of an infinite plane wall, in particular, were given in [14, Section 137]. In the 1970s the Lagrangian approach was applied by Hermans [15, Chapter 2] to study the stability of a translating gas bubble in an unbounded fluid under the influence of a step change in pressure. In the 1980s, Kok [16, 17] applied the method to study the motion of a pair of gas bubbles with constant radius in an unbounded fluid.

The present paper analyzes the forces exerted on, and the motion of a spherically deforming bubble in the vicinity of a plane infinite wall, occurring when capillary forces dominate inertial forces. Ideal-flow theory is applied since only bubbles at Reynolds numbers greater than 100 are considered. At these Reynolds numbers, the ratio of capillary to non-viscous hydrodynamic stresses, the Weber number, governs stability and bubble shape [18, 19]. The Lagrangian approach is used to derive the coupled equations of motion and deformation. Drag is accounted for by an extended Rayleigh dissipation function that enables us to account for the free-surface boundary layer. An alternative derivation of this equation will be given, and the R.P. equation will be extended to describe an imploding cavity moving in the vicinity of a wall. Moreover, a new solution method for the velocity potential that is systematic and applicable to general deformation will be introduced. The consistency of results obtained by the Lagrangian approach or by the Lagally theorem will be examined, and erroneous expressions derived by previous authors will be pointed out.

In Sections 2–5, the flow field and forces for an exanding spherical bubble in motion perpendicular to the wall will be studied. In Section 6, arbitrary motion of the center of mass will be considered. In Section 7, expressions for the drag forces for this case of general motion will be derived. Some examples of computed trajectories will be presented in Section 8.

2. Irrotational flow around a deforming bubble near a plane wall

In this section, added-mass coefficients and kinetic energy of the irrotational flow around an isotropically deforming bubble moving perpendicular to a plane wall are computed. In subsequent sections, the results will be used to compute the inertial and drag forces exerted on the bubble, the motion of the bubble centre induced by the expansion, and resulting trajectories. As explained in Section 1, such predictions can be used to analyze the growth of a boiling bubble near a hot plate. In the case of a rapidly growing boiling bubble, the free-surface boundary layer has a negligible contribution, and the use of ideal-fluid theory is appropriate. It will be assumed that capillary forces dominate inertial forces and that potential-flow theory can be applied.

The method introduced in this section to compute the harmonic velocity potential, ϕ, is a new systematic approach that can easily be applied to the case of arbitrary deformation of a bubble moving near a plane wall. The normal velocity at a point of the bubble interface, $\boldsymbol{x}_c$,

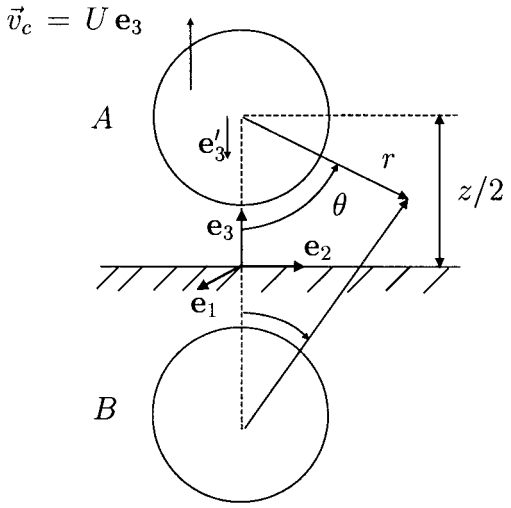

Figure 1. Coordinate systems and schematic of bubble system.

is[1] equal to the normal component of the liquid velocity, $\boldsymbol{v}$:

$$\boldsymbol{n} \cdot \frac{\mathrm{d}\boldsymbol{x}_c}{\mathrm{d}t} = \boldsymbol{n} \cdot \boldsymbol{v}(\boldsymbol{x}_c, t), \tag{1}$$

where $\boldsymbol{n}$ is the unit normal pointing into the liquid. For spherical deformation and velocity field describe by the potential ϕ, *i.e.*, $\boldsymbol{v} = \nabla\phi$, Equation (1) yields:

$$\left.\frac{\partial\phi}{\partial r}\right|_{r=R} = \dot{R} - U\,\cos\theta = \dot{R}\,P_o - U\,P_1(\cos\theta), \tag{2}$$

where R is the radius of the bubble, $\dot{R} \stackrel{\text{def}}{=} \partial R/\partial t$, (r, θ) is a spherical coordinate system centered at the bubble center that moves with the bubble-center velocity U away from the wall, as shown in Figure 1, and P_q is a Legendre polynomial of zeroth order. The usual approach to satisfy Equation (2) is to decompose the flow into two separate components expressing translation and expansion, and to sum the resulting two velocity potentials in order to get ϕ. In the case of arbitrary deformation the right-hand side of Equation (2) would require an infinite series of orthogonal polynomials, and the question whether the decomposition method yields a converging solution would arise. The method presented below is straightforward, avoids the need of decomposing into subproblems and answers intrinsically the question of convergence.

In the laboratory frame with Cartesian coordinate system $\{\mathbf{e}_i\}$ as shown in Figure 1 the wall is stationary. Let z be twice the distance of the bubble center from the plane wall. To simplify the algebra in the first few sections, the motion of the bubble is restricted to direction $\mathbf{e}_3$; in Section 6, the motion will be generalized. The wall is modeled by a mirror bubble, B, as shown in Figure 1. The flow field is described by a velocity potential, ϕ, that is comprised of two multipole expansions, one centered at the actual bubble, A, with coefficients $\{a_k\}$, and one centered at the mirror bubble, B, with the same coefficients for reasons of symmetry. With the aid of the shift formula [20], the flow potential is written for $r < z$ in terms of multipoles

[1]Here it is assumed that the ratio of the mass density of the vapor in the bubble, ρ_v, to that of the liquid, ρ_l, is much less than 1. This is the case in many boiling applications.

centered at A only:

$$\phi \;=\; \sum_{k=1}^{\infty} P_{k-1}(\cos\theta)\left\{a_k\, r^{-k} + \sum_{q=1}^{\infty}\binom{q+k-2}{k-1}\left(\frac{r}{z}\right)^{k-1} z^{-q}\, a_q\right\}. \tag{3}$$

Equation (3) is a general solution of the Laplace equation $\Delta\phi = 0$ for a system of two equal bubbles. For future reference, the set of coefficients $\{\tilde{a}_k\}$ is defined by

$$\tilde{a}_k \;=\; R^{-k}\, a_k. \tag{4}$$

Let $l^2(\phi)$ denote the Hilbert space of the real coefficients $(a_1,\ a_2,\ a_3,\ \ldots)$ satisfying $\sum_{i=1}^{\infty} a_i^2 < \infty$. To solve for $(a_1,\ a_2,\ a_3,\ \ldots)$, it is expedient to define the compact operator $\mathbf{F}$ on $l^2(\phi)$ with the aid of the matrix representation using the standard orthonormal basis:

$$F_{i\,j} \;\stackrel{\text{def}}{=}\; -\delta_{i\,j} + \frac{i-1}{i}\, R^{2i-1}\, z^{-i-j+1}\binom{i+j-2}{i-1}, \tag{5}$$

where δ_{ij} denotes the Kronecker delta. Since the Legendre polynomials are orthogonal, the boundary condition (2) requires

$$\sum_{j=1}^{\infty} F_{i\,j}\, a_j \;=\; R^2\,\dot{R}\,\delta_{i1} - \tfrac{1}{2}\, R^3\, U\,\delta_{i2}. \tag{6}$$

Let the case that both $\dot{R} = 0$ and $U = 0$ be considered as trivial and excluded from the analysis. Define $\boldsymbol{\alpha}$ by $\boldsymbol{\alpha} \stackrel{\text{def}}{=} \mathbf{F} + \mathbf{I}$ with $I_{ij} \stackrel{\text{def}}{=} \delta_{ij}$. A sufficient condition for $\mathbf{F}$ to have an inverse is that $\boldsymbol{\alpha}$ is a Hilbert–Schmidt operator, *i.e.*, $\sum_{i,j=1}^{\infty} \left|\alpha_{i\,j}\right|^2 < \infty$, for the following reason. Suppose that $\boldsymbol{\alpha}$ is a Hilbert-Schmidt operator. Each Hilbert–Schmidt operator is compact; according to the Fredholm alternative either 1 is an eigenvalue of $\boldsymbol{\alpha}$, or $\boldsymbol{\alpha} - \mathbf{I}$ has an inverse. If 1 would be an eigenvalue of $\boldsymbol{\alpha}$, then a non-zero element $\{a_i\}$ of $l^2(\phi)$ would exist, such that $\sum_{j=1}^{\infty} \alpha_{1\,j}\, a_j - a_1$ would be equal to zero. Because of Equation (6), this can not be the case if $R^2\,\dot{R}$ or $R^3\,U$ is selected to be non-zero. If therefore the trivial case (both $\dot{R} = 0$ and $U = 0$) is excluded from the analysis, 1 is not an eigenvalue of $\boldsymbol{\alpha}$. According to the Fredholm alternative, $\boldsymbol{\alpha} - \mathbf{I}$ has an inverse. This means that $\mathbf{F}$ has an inverse if $\boldsymbol{\alpha}$ is a Hilbert-Schmidt operator[2].

Is is shown in Appendix 9 that rescaling might be required for $\boldsymbol{\alpha}$ to be a Hilbert-Schmidt operator, but that an operator $\mathbf{G}$ can be defined, based on the set $\{\tilde{a}_k\}$ rather than on $\{a_k\}$, whose inverse unconditionally exists and which only depends on (R/z).

Equation (6) yields

$$a_j \;=\; F_{j1}^{-1}\, R^2\,\dot{R} - \tfrac{1}{2}\, R^3\, U\, F_{j2}^{-1}. \tag{7}$$

[2]Note that if $\boldsymbol{\alpha}$ is a Hilbert–Schmidt operator, $\mathbf{F}$ has a kernel, as is a requirement for the numerical boundary-element method (not applied here) to be applicable.

To solve the infinite set of equations, the method of reduction [21] is used. In case of Equation (7) this implies that all a_j with $j > n$ are put equal to zero, and $\mathbf{F}^{-1}$ is determined with the aid of Equation (5). Since the linear space spanned by the basis vectors is dense in $l^2(\phi)$, the solution $\tilde{a}$ of Equation (7) is in this way approximated with an arbitrary degree of accuracy. Sample computations are given in Section 8.

In the remainder of this section, expressions for the added-mass coefficients will be derived. In order to simplify the expressions of the added-mass coefficient and the kinetic energy of the fluid, and also to facilitate comparison with the Lagally theorem in Section 4, the following property of the operator $\mathbf{F}^{-1}$ is derived in Appendix 9:

$$F^{-1}_{i\,j}\left(\frac{j-1}{j}\right) R^{2j-1} \;=\; F^{-1}_{j\,i}\left(\frac{i-1}{i}\right) R^{2i-1}. \tag{8}$$

One of the important consequences of Equation (8) is that

$$F^{-1}_{(i+1)1} \;=\; \left(\sum_{l=2}^{\infty} z^{-l}\, F^{-1}_{l(i+1)}\right) \frac{i}{i+1}\, R^{2i+1}, \tag{9}$$

as proved in Appendix 9.

An immediate consequence of Equation (7) is that the velocity potential ϕ is the sum of two parts:

$$\phi = \boldsymbol{v}_c \cdot \boldsymbol{\Phi} + \dot{R}\ \chi, \tag{10}$$

where

$$\begin{aligned}\vec{\Phi} \;=\; \mathbf{e}_3\,\Phi_3 \;&\stackrel{\text{def}}{=}\; -\mathbf{e}_3\,\tfrac{1}{2}\,R^3\Bigg[\sum_{i=1}^{\infty} F^{-1}_{i2}\, r^{-i}\, P_{i-1} + \\ &+\sum_{j,k=1}^{\infty} F^{-1}_{j2}\, z^{-j-k+1}\binom{k+j-2}{k-1} r^{k-1}\, P_{k-1}\Bigg],\end{aligned} \tag{11a}$$

$$\chi = R^2\left[\sum_{i=1}^{\infty} F^{-1}_{i1}\, r^{-i}\, P_{i-1} + \sum_{j,k=1}^{\infty} F^{-1}_{j1}\, z^{-j-k+1}\binom{k+j-2}{k-1} r^{k-1}\, P_{k-1}\right]. \tag{11b}$$

The kinetic energy, T, of the fluid in the halfspace comtaining bubble A and bounded by the wall is given by

$$T \;=\; -\tfrac{1}{2}\,\rho_l \iint_A \phi\,(\boldsymbol{v}_c \cdot \boldsymbol{n} + \dot{R})\ \mathrm{d}S, \tag{12}$$

where $\boldsymbol{n}$ is the outward normal to the bubble, $\boldsymbol{n} = \sum_{i=1}^{3} n_i \mathbf{e}_i$.

Dimensionless added-mass tensors are defined by:

$$\alpha_{i\,j} \;\stackrel{\text{def}}{=}\; -\frac{1}{\mathcal{V}_b}\iint \Phi_j\, n_i\ \mathrm{d}S, \tag{13a}$$

$$\beta_{i\,j} \stackrel{\text{def}}{=} -\frac{1}{\mathcal{V}_b}\iint \chi\, n_i\, n_j\ \mathrm{d}S, \tag{13b}$$

$$\psi_i \stackrel{\text{def}}{=} -\frac{1}{\mathcal{V}_b}\iint (\Phi_i + n_i\,\chi)\ \mathrm{d}S, \tag{13c}$$

where $\mathcal{V}_b$ denotes the volume of the bubble. Equations (10), (12), and (13) combine to give

$$\frac{2\,T}{\rho_l} = \mathcal{V}_b\,\alpha_{3\,3}\,U^2 + \mathcal{V}_b\,\dot{R}^2\,\mathrm{tr}(\beta) - \mathcal{V}_b\,\dot{R}\,U\,\psi_3, \tag{14}$$

where tr(β) is the trace of $\boldsymbol{\beta}$. The integrations in Equation (13a) are straightforward. With the aid of Equations (9) and (15):

$$F_{11}^{-1} = -1 \text{ and } F_{12}^{-1} = 0, \tag{15}$$

these integrations yield

$$\alpha_{3\,3} = -1 - \tfrac{3}{2}\,F_{22}^{-1} = -1 - \tfrac{3}{2}\,G_{22}^{-1}, \tag{16a}$$

$$\mathrm{tr}(\beta) = 3 - 3\,R\sum_{k=1}^{\infty} F_{k\,1}^{-1}\,z^{-k} = 3 - 3\sum_{k=1}^{\infty} G_{k\,1}^{-1}\left(\frac{R}{z}\right)^k, \tag{16b}$$

$$\psi_3 = -6\,R^{-1}\,F_{21}^{-1} = -6\,G_{21}^{-1}, \tag{16c}$$

where the coefficients G_{ij}^{-1} are defined in Appendix 9, and show that the added-mass coefficients are functions of the ratio (R/z) only. Expressions (16) for the added-mass coefficients of a radially expanding sphere near a plane wall are new. Results obtained using these will be compared in Section 4 with results of the literature.

3. The acceleration of the bubble center

The instantaneous velocity of the center of the bubble, $\boldsymbol{v}_c$, is given by $U\,\mathbf{e}_3$. In order to be able to predict bubble motion starting from a given initial distance from the wall, $z/2$, radius, R, growth rate, $\dot{R}$, and velocity, U, the acceleration $\dot{U}$ has to be determined. The Lagrange–Thomson approach is applied.

Let $z/2$ be the first generalized coordinate, q_1, and let $q_2 \stackrel{\text{def}}{=} R$. The corresponding generalized velocities $(U,\ \dot{R})$ are assumed to be known at a given instant of time. Let Q_j be the generalized forces exerted on the fluid, and let conservative forces be part of the Q_j. The two coordinates $\{q_i\}$ satisfy the requirements that all working agents are included in $\sum_{i=1}^{2} Q_i\,\dot{q}_i$, and that $Q_1\,\dot{q}_1$ is independent of $Q_2\,\dot{q}_2$. The generalized forces are given by

$$Q_j = \frac{\mathrm{d}}{\mathrm{d}t}\frac{\partial T}{\partial \dot{q}_j} - \frac{\partial T}{\partial q_j}. \tag{17}$$

Without loss of generality, conservative forces (gravity) are left out of the analysis to simplify the writing. Taking the pressure at infinity homogeneous and constant in time, the hydrodynamic force on the bubble in $\mathbf{e_3}$-direction, F_3, is given by $-Q_1$. Since the liquid is incompressible, Equation (17) divided by ρ_l yields

$$\frac{F_3}{\rho_l} = -\frac{\mathrm{d}}{\mathrm{d}t}\frac{\partial(T/\rho_l)}{\partial U} + 2\frac{\partial(T/\rho_l)}{\partial z} \tag{18}$$

with T/ρ_l given by Equations (14) and (16a). The first term on the right-hand side of Equation (18) is the acceleration reaction, and is equal to

$$\frac{\mathrm{d}}{\mathrm{d}t}\left[U\mathcal{V}_b + \tfrac{3}{2}\mathcal{V}_b U F_{22}^{-1} - 4\pi R^2 F_{21}^{-1}\dot{R}\right] \tag{19}$$

The second term on the right-hand side of Equation (18) is the steady motion acceleration, and is given by

$$U^2\mathcal{V}_b\frac{\partial\alpha_{33}}{\partial z} + \dot{R}^2\mathcal{V}_b\frac{\partial \mathrm{tr}(\beta)}{\partial z} - \dot{R}U\mathcal{V}_b\frac{\partial\psi_3}{\partial z}. \tag{20}$$

To compute $\partial\alpha_{33}/\partial z$, Equation (8) is used, yielding:

$$\frac{\partial F_{22}^{-1}}{\partial z} = \sum_{i,j=1}^{\infty} -F_{2i}^{-1}\frac{\partial F_{ij}}{\partial z}F_{j2}^{-1} = \sum_{i,j=1}^{\infty}\tfrac{1}{2}R^3 z^{-i-j}\frac{(i+j-1)!}{(i-1)!\,(j-1)!}F_{j2}^{-1}F_{i2}^{-1}. \tag{21}$$

In a similar fashion, the steady-motion acceleration can be shown to be the sum of (22), (23) and (24):

$$-\sum_{i,j=1}^{\infty} U^2 R^6\pi\frac{(i+j-1)!}{(i-1)!\,(j-1)!}z^{-i-j}F_{i2}^{-1}F_{j2}^{-1}, \tag{22}$$

$$-\sum_{k,n=1}^{\infty}\dot{R}U4\pi R^5\frac{(k+n-1)!}{(k-1)!\,(n-1)!}z^{-k-n}F_{k1}^{-1}F_{n1}^{-1}, \tag{23}$$

$$-\sum_{i,j=1}^{\infty}\dot{R}^2 4\pi R^4\frac{(i+j-1)!}{(i-1)!\,(j-1)!}z^{-i-j}F_{i1}^{-1}F_{j1}^{-1}, \tag{24}$$

respectively corresponding to the U^2-term, the $\dot{R}U$-term and the $\dot{R}^2$-term, $\dot{R}^2\mathcal{V}_b\,\partial\mathrm{tr}(\beta)/\partial z$, of Equation (20). Since the total force is given by

$$\begin{aligned}-\frac{F_3}{\rho_l} = {} & \alpha_{33}\dot{U}\mathcal{V}_b - \tfrac{1}{2}\psi_3\ddot{R}\mathcal{V}_b + U\dot{R}\left\{\mathcal{V}_b\frac{\partial\alpha_{33}}{\partial R} + 4\pi R^2\alpha_{33}\right\} + \\ & + U^2\mathcal{V}_b\frac{\partial\alpha_{33}}{\partial z} - \tfrac{1}{2}\dot{R}^2\left\{\mathcal{V}_b\frac{\partial\psi_3}{\partial R} + 2\mathcal{V}_b\frac{\partial\mathrm{tr}(\beta)}{\partial z} + 4\pi R^2\psi_3\right\}\end{aligned} \tag{25}$$

and since

$$\mathcal{V}_b\frac{\partial\psi_3}{\partial R} + 4\pi R^2\psi_3 = -24\pi R^2\frac{\partial F_{21}^{-1}}{\partial R}, \tag{26}$$

an algebraic expression for F_3, in terms of known parameters and $\dot{U}$ and $\ddot{R}$, is obtained once Equation (21) is substituted, as well as algebraic expressions for the derivatives $\partial F_{21}^{-1}/\partial R$ and $\partial \alpha_{33}/\partial R$. These expressions are derived using Equation (8), which yields:

$$\frac{\partial F_{21}^{-1}}{\partial R} \;=\; -\sum_{i,j=1}^{\infty} \tfrac{1}{2}\, R^2\,(2i-1)\, z^{-i-j+1} \binom{i+j-2}{i-1} F_{i2}^{-1}\, F_{j1}^{-1}, \tag{27}$$

$$\frac{\partial F_{22}^{-1}}{\partial R} \;=\; -\sum_{i,j=1}^{\infty} \tfrac{1}{2}\, R^2\,(2i-1)\, z^{-i-j+1} \binom{i+j-2}{i-1} F_{i2}^{-1}\, F_{j2}^{-1}. \tag{28}$$

Evaluation of the velocity potential and the hydrodynamic force F_3 is a simple task using the program Matlab™, the definition of $\mathbf{F}$ given by Equation (5), Equation (25) and the algebraic expressions (21)–(24) and (26)–(28).

For use in Section 5 the following derivative is given:

$$\frac{1}{3}\frac{\partial \mathrm{tr}(\beta)}{\partial R} \;=\; \sum_{j=1}^{\infty} z^{-j}\, F_{j1}^{-1} + \sum_{i,j=1}^{\infty} F_{i1}^{-1}\,(2i-1)\, z^{-i-j+1} \binom{i+j-2}{i-1} F_{j1}^{-1}. \tag{29}$$

In order to compare the present results with the results of previous authors, the expressions derived earlier in this section will now be simplified for an asymptotic case.

With the aid of Equations (5) and (6) it can be shown that

$$a_2 \;=\; \tfrac{1}{2}\, R^3\, h_1\,(U - R^2\,\dot{R}\, z^{-2}) + \tfrac{1}{2}\, R^3\, h_1\, z^{-2} \sum_{j=3}^{\infty} j\, a_j\, z^{1-j} \tag{30}$$

with

$$h_1 \;\stackrel{\text{def}}{=}\; \frac{1}{1-(R/z)^3}. \tag{31}$$

Far from the wall, for values of z/R to be specified below, the higher order multipole contributions are negligible compared to a_1 and a_2. A comparison of Eq (30) with (7) shows that

$$\text{if } a_3 \;=\; a_4 \;=\; \ldots \;=\; 0 \text{ then } F_{22}^{-1} \;\sim\; -h_1 \text{ and } F_{21}^{-1} \;\sim\; -\tfrac{1}{2}\, h_1\, R\, y^2, \tag{32}$$

where y, as defined by

$$y \;\stackrel{\text{def}}{=}\; R/z \tag{33}$$

is $\frac{1}{2}$ at maximum. The approximation may be summarised as follows:

$$-\frac{F_3}{\rho_l} \approx \dot{R}^2\, R^2\, y^2\, \pi\,(4 - 10\, h_1) + \dot{R}\, U\, R^2\, \pi\,(6\, h_1 - 4) + \dot{U}\, R^3\, \pi\, \left(2\, h_1 - \tfrac{4}{3}\right) + \\ + \ddot{R}\,(-2\,\pi\, h_1\, R^3\, y^2) - 6\,\pi\, R^2\, h_1^2\, U^2\, y^4. \tag{34}$$

Equations (32) and (16a) show that the added mass α_{33} is $\frac{1}{2}$ at large distances from the wall. Also, the results of Thomson and Tait [14, Section 137] are easily recovered in this way. In the approximation of Equation (32), the added-mass coefficients are given by:

$$\alpha_{33} \;\sim\; \tfrac{3}{2}\, h_1 - 1, \quad \mathrm{tr}(\beta) \;\sim\; 3 + 3\, y + \tfrac{3}{2}\, h_1\, y^4, \quad \psi_3 \;\sim\; 3\, y^2. \tag{35a}$$

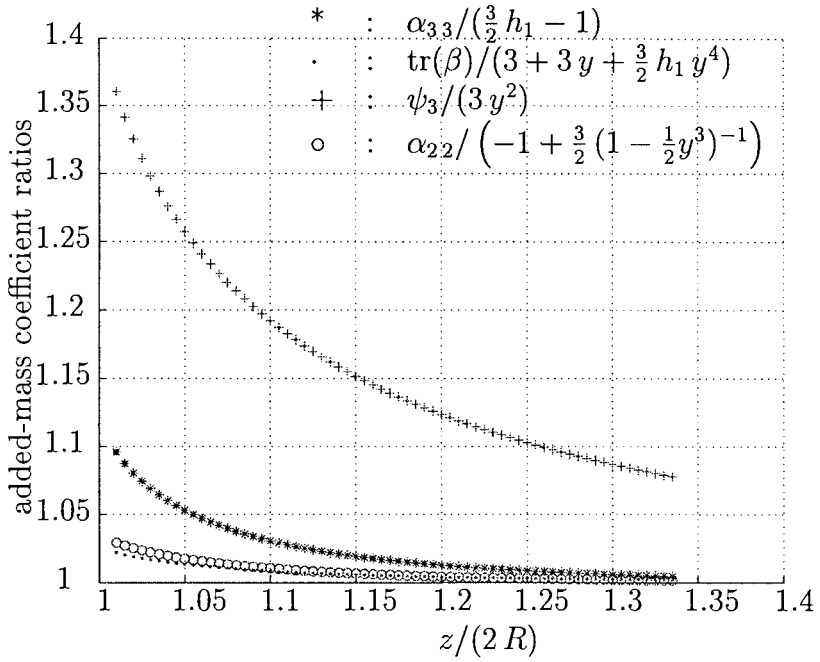

Figure 2. Ratios of added-mass coefficients to approximated values, given by Equations (35a) and (64), in the vicinity of the wall.

Figure 2 shows that Equation (35a) are accurate to within 1% for $(\frac{1}{2}z/R) > 1{\cdot}4$.

Voinov [22] derived an exact expression of T for two touching solid spheres, *i.e.*, for $y = \frac{1}{2}$:

$$T(y = \tfrac{1}{2},\ \dot{R} = 0) \ = \ \tfrac{1}{4}\,\rho_l\,\mathcal{V}_b\ (3 \cdot \zeta(3) - 2)\ U^2, \tag{36}$$

where ζ is the Riemann ζ-function; $\zeta(3) \sim 1{\cdot}202060$. Solving Equation (16a) in this case requires at least 80 coefficients for $z/(2\,R) = 1{\cdot}01$; linear extrapolation of the ratio $\alpha_{33}/(\frac{3}{2}\,h_1 - 1)$, see Figure 2, gives $\alpha_{33} \approx 0{\cdot}8$, which equals $\frac{1}{2}(3{\times}1{\cdot}2{-}2)$ and is therefore practically identical to $\frac{1}{2}(3\zeta(3) - 2)$.

Witze *et al.* [23] used bipolar coordinates to solve the problem of an isotropically expanding sphere that remains attached to the wall. In this case, $U = \dot{R}$, and taking $R = \varepsilon\,t^{1/2}$ they computed

$$T(y = \tfrac{1}{2},\ U = \dot{R}) \ \approx \ 9{\cdot}33\,\rho_l\,\dot{R}^2\,R^3, \tag{37a}$$

$$F_3(y = \tfrac{1}{2},\ U = \dot{R}) \ \approx \ -0{\cdot}29\,\pi\,\varepsilon^4\,\rho_l. \tag{37b}$$

The coefficients 9·33 and 0·29 of Equation (37) are in good agreement with those computed with Equations (14) and (25): 9·35 and 0·28 respectively. Since the convergence of the series involved is slowest for $y = \frac{1}{2}$, and since the predictions appear to be good for the two extremes $y = \frac{1}{2}$ and for $y \ll 1$, the results are expected to be correct for each y-value in $(0,\ \frac{1}{2})$.

Miloh *et al.* [24] considered several related cases, including a stationary expanding sphere near a plane wall and a rigid sphere moving near a plane wall, by using the Lagally theorem. Miloh accounted for the dipole terms related to translational motion of the center, but those related to the expansion ($\tilde{D}_1$ in his terminology) appear to be missing. Since $\tilde{D}_1$ does not

occur in the acceleration reaction in his Equation (15a), his Equation (80) for the force on a stationary sphere near a wall seems to be missing a term proportional to the acceleration $\ddot{R}$.

4. Comparison with the Lagally theorem

In Section 3, the Lagrangian approach was applied to an expanding bubble, thereby extending Lamb's work to deformable systems. To validate our results, we compare them to those obtained by direct methods where the pressure is evaluated using Bernoulli's equation. A convenient way to do this is to apply the Lagally theorem derived by M. Lagally, G.I. Taylor and others originally in the 1920's. In the 1950's and 1980's, Landweber *et al.* [25] and Landweber *et al.* [26] extended the theorem, to include deformation. Van Wijngaarden [27] and Biesheuvel [28] simplified the derivation of the generalized Lagally theorem.

According to the Lagally theorem, the hydrodynamic force on the bubble, $\boldsymbol{F}$, is given by

$$\frac{1}{\rho_l}\boldsymbol{F} = \frac{\mathrm{d}}{\mathrm{d}t}\left[\frac{\mathrm{d}}{\mathrm{d}t}\,(\boldsymbol{x}_c\,\mathcal{V}_b) - 4\,\pi \sum_{\text{monopoles}} p_o\; D^o\big|_s\,(\boldsymbol{x}) - 4\,\pi \sum_{\text{dipoles}} p_1\, D^1\big|_s\,(\boldsymbol{x})\right] + \\ -4\,\pi \sum_{\text{singularities}} p_q^s\, D^q\big|_s\,\boldsymbol{v}'. \qquad (38)$$

The following definitions are used in Equation (38):

$s \quad \stackrel{\text{def}}{=}$ number of the singularity, situated at $\boldsymbol{x}_s$,

$\boldsymbol{v}'(\boldsymbol{x}) \quad \stackrel{\text{def}}{=}$ the velocity induced at $\boldsymbol{x}$ minus the velocity, induced at $\boldsymbol{x}$ by multipoles situated at $\boldsymbol{x}$,

$D^0 \quad \stackrel{\text{def}}{=}$ I ,

$p_o \quad \stackrel{\text{def}}{=}$ negative of the strength of the monopole.
If $\phi_d = -\dfrac{m_s}{r}$ with $r \stackrel{\text{def}}{=} |\boldsymbol{x} - \boldsymbol{x}_s|$, $p_o\; D^0|_s(\boldsymbol{x}) = m_s\, \boldsymbol{x}_s$,

$p_1^i \quad \stackrel{\text{def}}{=}$ strength of dipole-component i.

$p_1\; D^1|_s(\boldsymbol{x}) \quad \stackrel{\text{def}}{=} \displaystyle\sum_i p_1^i\, \frac{\partial}{\partial x^i}\bigg|_s \boldsymbol{x} = \sum_i p_1^i\, \mathbf{e}_i = \boldsymbol{p}_1.$
If $\phi = \vec{\mu}\cdot\nabla\dfrac{1}{r} = -r^{-3}\,\vec{\mu}\cdot\boldsymbol{r}$, then $p_1\, D^1|_s(\boldsymbol{x}) = \vec{\mu}$,

$p_2^{ij} \quad \stackrel{\text{def}}{=}$ strength of quadropole-moment (i, j) ,

$p_2\; D^2|_s(\boldsymbol{v}) \quad \stackrel{\text{def}}{=} \displaystyle\sum_i\sum_j p_2^{ij}\frac{\partial}{\partial x^i}\frac{\partial}{\partial x^j}\bigg|_s (\boldsymbol{v})$.
If $\phi = -(-1)^q p_q\; D^q\,\dfrac{1}{r}$, then
$p_q D^q|_s(\boldsymbol{v}) = \displaystyle\sum_i\sum_j\sum_k p_q^{ijk\ldots}\frac{\partial}{\partial x^i}\;\frac{\partial}{\partial x^j}\;\frac{\partial}{\partial x^k}\cdots\bigg|_s\;(\boldsymbol{v})$,

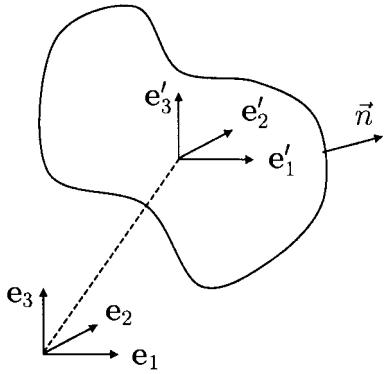

Figure 3. Definition of moving (primed) and laboratory reference systems

$\mathcal{V}_b \stackrel{\text{def}}{=}$ the volume of the object (bubble),

$\boldsymbol{v}_c \stackrel{\text{def}}{=}$ the velocity of the center of the object, situated at $\boldsymbol{x}_c$,

$\rho_l \stackrel{\text{def}}{=}$ the mass density of the fluid.

However, Landweber and Miloh [26] and Biesheuvel [28] derived *two* expressions for the force on an expanding bubble. In their other expression, the acceleration reaction, the first term on the RHS of Equation (38), was written as

$$\frac{\mathrm{d}}{\mathrm{d}t}\left[\boldsymbol{v}_c\,\mathcal{V}_b - 4\,\pi \sum_{\text{singularities}} p_q^s\, D^q\big|_s\,(\boldsymbol{x}) + \frac{\mathrm{d}}{\mathrm{d}t}\,(\boldsymbol{x}_c\,\mathcal{V}_b)\right]. \tag{39}$$

It will now be shown that expression (39) is wrong, and that the differences with the proper expression for $\boldsymbol{F}$ are only apparent if expansion or contraction takes place. It will be be shown that the deformation monopoles do not contribute to the acceleration reaction. Finally, it will be shown that the force predicted in Section 3 is identical to the force predicted by the Lagally theorem.

First, an alternative expression for $\boldsymbol{F}$ is derived, starting from Equation (38). Let $\mathbf{e}_i$ be a unit vector in a Cartesian laboratory frame and $\mathbf{e}'_i$ a unit vector in a Cartesian body-fixed coordinate system, see Figure 3. By definition, $\boldsymbol{x}' = \boldsymbol{x} - \boldsymbol{x}_c$, where $\boldsymbol{x}_c$ is the body's centroid, defined by

$$\boldsymbol{x}_c = \frac{1}{\mathcal{V}_b}\iiint \boldsymbol{x}\;\mathrm{d}\mathcal{V}. \tag{40}$$

The velocity of a point at the surface of the deformable body, $\boldsymbol{u}$, can be decomposed as

$$\boldsymbol{u} = \boldsymbol{v}_c + \boldsymbol{v}_d, \tag{41}$$

where $\boldsymbol{v}_c = \mathrm{d}\boldsymbol{x}_c/\,\mathrm{d}t$ is the velocity of the body's centroid. It is shown in Appendix 9 that

$$\frac{\mathrm{d}}{\mathrm{d}t}\,(x_{c,i}\,\mathcal{V}_b) = \iint x_i\,\boldsymbol{v}_d\cdot\boldsymbol{n}\;\mathrm{d}S + \boldsymbol{v}_c\cdot\iint x_i\,\boldsymbol{n}\;\mathrm{d}S. \tag{42}$$

Here $\boldsymbol{n}$ is the outward normal to the surface. Equation (42) disagrees with expression (48) given by Landweber *et al.* [26, pg. 39]. In Appendix 9 it is shown that

$$\iint x'_i\,\boldsymbol{v}_d\cdot\boldsymbol{n}\;\mathrm{d}S = 0, \tag{43}$$

which is equivalent to Equation (5) of Saffman [29]. Equation (43) is now used to prove

$$\boldsymbol{v}_c\,\mathcal{V}_b - 4\,\pi \sum_{\text{singularities}}^{\not d} p_q^s\, D^q(\boldsymbol{x})_s + \iint \phi_d\,\boldsymbol{n}\,\mathrm{d}S \;= \\ = \frac{\mathrm{d}}{\mathrm{d}t}\,(\boldsymbol{x}_c\,\mathcal{V}_b) - 4\,\pi \sum_{\text{singularities}} p_q^s\, D^q(\boldsymbol{x})_s. \tag{44}$$

The $\not d$ superscript implies that the summation does not extend to the multipoles that are related to the deformation potential, ϕ_d, and the suffix d denotes deformation.

If the velocity potential ϕ is expanded as

$$\phi \;=\; \cdots - \frac{m}{r} + \vec{\mu}\cdot\nabla\frac{1}{r} + \sum_{i,j=1}^{3} p_2^{ij}\,\frac{\partial}{\partial x_i}\,\frac{\partial}{\partial x_j}\,\frac{1}{r} + \cdots,$$

then the monopole strength, m, and the dipole strength, $\vec{\mu}$, can be expressed as integrals over ϕ and $\boldsymbol{n}\cdot\nabla\phi$ ([30, p. 121]). Equation (43) then yields

$$\iint \phi_d\,\boldsymbol{n}\,\mathrm{d}S \;=\; -4\,\pi\,\vec{\mu}_d, \tag{45}$$

$$\iint \boldsymbol{x}\,\boldsymbol{v}_d\cdot\boldsymbol{n}\,\mathrm{d}S \;=\; 4\,\pi\,m_d\,\boldsymbol{x}_c. \tag{46}$$

Here m_d and μ_d are the monopole and dipole strengths in the expansion of ϕ_d, respectively. Equations (46) and (42) give

$$\boldsymbol{v}_c\,\mathcal{V}_b \;=\; \frac{\mathrm{d}}{\mathrm{d}t}\,(\boldsymbol{x}_c\,\mathcal{V}_b) - 4\,\pi\,m_d\,\boldsymbol{x}_c. \tag{47}$$

Equations (45) and (47) prove Equation (44).

With the aid of Equation (44) it can be sown that the force $\boldsymbol{F}$ on an expanding bubble is alternatively given by

$$\frac{1}{\rho_l}\boldsymbol{F} \;=\; \frac{\mathrm{d}}{\mathrm{d}t}\left[\boldsymbol{v}_c\,\mathcal{V}_b - 4\,\pi \sum_{\text{monopoles}}^{\not d} p_o\;\; D^o\big|_s\,(\boldsymbol{x}) - 4\,\pi\sum_{\text{dipoles}}^{\not d} p_1\, D^1|_s(\boldsymbol{x}) + \iint \phi_d\,\boldsymbol{n}\,\mathrm{d}S\right] + \\ - 4\,\pi \sum_{\text{singularities}} p_q^s\, D^q\big|_s\,\boldsymbol{v}' \tag{48}$$

and that the term $\boldsymbol{v}_c\,\mathcal{V}_b$ should be omitted from Equation (39). If this term were retained, $\boldsymbol{F}/\rho_l$ would contain $\mathrm{d}\,(2\boldsymbol{v}_c\,\mathcal{V}_b)\,/\,\mathrm{d}t$, which would yield a $\dot{U}$-term twice as big as it should be.

Equations (48)and (45) show that *only the dipole* of the deformation potential contributes to the acceleration reaction. The monopole contribution corresponding to ϕ_d in Equation (44) is balanced by $\boldsymbol{x}_c\;\mathrm{d}\mathcal{V}_b/\,\mathrm{d}t$.

It will now be shown that the Lagally theorem yields the same force on the bubble as that obtained by the Lagrangian approach.

Using the proper expression for the Lagally theorem, it can be shown that F_3 is given by

$$\frac{F_3}{\rho_l} \;=\; \frac{\mathrm{d}}{\mathrm{d}t}\,[U\,\mathcal{V}_b - 4\,\pi\,a_2] - 4\,\pi\sum_{n=1}^{\infty} n\,a_n \sum_{k=1}^{\infty} a_k \binom{k+n-1}{n-1} z^{-n-k}. \tag{49}$$

The a_i-coefficients are now expressed in F_{ij}-elements with the aid of (7). This yields for the acceleration due to steady motion the sum of (22), (23), and (24). Equation (7) shows that the acceleration reaction is given by (19). The force computed with the Lagally theorem (38) is therefore the same as that predicted by the Lagrangian approach. In Section 5, the latter approach will be seen to additionally yield an extended Rayleigh equation.

5. A generalized Rayleigh equation

One particular advantage of the Lagrange-Thomson approach is that the governing equation for $\ddot{R}$ comes out naturally from the Lagrangian equation corresponding to the radius R. This extended Rayleigh–Plesset equation will now be derived.

The generalized force on the bubble, F_R, corresponding to isotropic expansion is derived using the kinetic energy given by Equation (14), the added-mass coefficients given by (16a), and the derivatives given by (21), (24), and (26)–(29). The result is

$$\begin{aligned}\frac{F_R}{\rho_l} \;=\; & \ddot{R}\,4\,\pi\,R^3\left\{-1+\sum_{k=1}^{\infty} R\,z^{-k}\,F_{k1}^{-1}\right\}-\dot{U}\,4\,\pi\,R^2\,F_{21}^{-1}+2\,\pi\,R^2\,\dot{R}^2\left\{-3+\right.\\ & \left.+3\,R\sum_{m=1}^{\infty} z^{-m}\,F_{m1}^{-1}-\sum_{i,j=1}^{\infty} R\,z^{1-i-j}\,(2i-1)\binom{i+j-2}{i-1}F_{i1}^{-1}\,F_{j1}^{-1}\right\}+\\ & +\sum_{l,m=1}^{\infty} 8\,\pi\,R^3\,U\,\dot{R}\,R\,z^{-l-m}\binom{l+m-2}{l-1}(l+m-1)\,F_{l1}^{-1}\,F_{m1}^{-1}+\\ & -\sum_{i,j=1}^{\infty} U^2\,4\,\pi\,R^5\,z^{-i-j}\binom{i+j-2}{i-1}(i+j-1)\,F_{j1}^{-1}\,F_{i2}^{-1}+\\ & -U^2\,\pi\,R^2\left\{2+3\,F_{22}^{-1}-\sum_{i,j=1}^{\infty}\tfrac{1}{2}\,R^3\,z^{-i-j+1}\,(2i-1)\binom{i+j-2}{i-1}F_{i2}^{-1}\,F_{j2}^{-1}\right\}. \end{aligned}\tag{50}$$

The approximation (32) yields

$$\begin{aligned}\frac{F_R}{2\,\pi\,R^2\,\rho_l} \;\approx\; & -\ddot{R}\,R\,(2+2\,y+y^4\,h_1)-\dot{R}^2\left(3+4\,y+\tfrac{7}{2}\,y^4\,h_1+\tfrac{3}{2}\,y^7\,h_1^2\right)+\\ & +\dot{U}\,R\,y^2\,h_1+U\,\dot{R}\,(4\,y^2+8\,y^5\,h_1+6\,y^8\,h_1^2)+\\ & +U^2\left(\tfrac{3}{2}\,h_1-1+\tfrac{3}{2}\,y^3\,h_1^2-4\,y^3\,h_1-6\,y^6\,h_1^2\right). \end{aligned}\tag{51}$$

Zijl [6, Chapter 18, p. 568] truncated an expansion of the velocity potential after y^2, applied the Bernoulli equation and direct integration of the pressure. By comparing terms proportional to $\cos(\theta)$ he was able to derive the terms $-\ddot{R}\,R\,(2+2\,y)-\dot{R}^2\,(3+4\,y)$. Equation (51) will now be used to derive an extended version of what is known as the Rayleigh-Plesset equation, that dates from 1917 (Rayleigh) and 1949 (Plesset) and applies to a bubble in an unbounded fluid. This equation is usually derived by integration of the Navier-Stokes equations, see for example Brennen [5]. The approach followed here is, in the view of the author, more elegant and applies to a bubble in the vicinity of a plane, infinite wall. Since viscous dissipation is intrinsic in Navier-Stokes flow, it has to be accounted for. This is done with the aid of the Levich approach that is more fully discussed in Section 7.

The derivation starts with identifying the generalized forces involved, by computing the power provided at the bubble boundary. Consider a system of two identical spherical bubbles surrounded by liquid. The time rate of change of kinetic energy of the liquid, T_{A+B}, in the volume outside the two bubbles is given by

$$\frac{\mathrm{d}T_{A+B}}{\mathrm{d}t} \;=\; \sum_{j=1}^{N} Q_j \dot{q}_j \tag{52}$$

Integration of the mechanical energy equation [31, Section 3.3], and application of the Leibniz theorem (see Appendix 9) yields for an incompressible liquid

$$\frac{\mathrm{d}T_{A+B}}{\mathrm{d}t} = \iint p_l \, \boldsymbol{n}\cdot\boldsymbol{v} \; \mathrm{d}S - \dot{\Phi} + \iiint \rho \, \boldsymbol{v}\cdot\vec{g} \; \mathrm{d}\mathcal{V} + \iint \boldsymbol{n}\cdot\vec{\vec{\tau}}\cdot\boldsymbol{v} \; \mathrm{d}S, \tag{53}$$

where $\dot{\Phi}$ is the total energy dissipation rate in the liquid volume outside the two bubbles, p_l is the pressure in the liquid, $\boldsymbol{n}$ is the normal pointing into the liquid, $\vec{g}$ is the gravity vector, and the last term represents viscous traction at the boundaries of the bubble and at infinity. If the velocity field at infinity is homogeneous, the traction term is only nonzero at the bubble surface, where it can be written as

$$-\dot{R}\, 2\,\mu_l \iint_A \frac{\partial v_{l,r}}{\partial r} \; \mathrm{d}S$$

with $v_{l,r}$ the normal liquid velocity component and μ_l the dynamic viscosity of the liquid. Without loss of generality, gravity is left out of the analysis to simplify the writing. Taking the pressure at infinity constant and equal to $p_{l,\infty}$, Equations (52) and (53) yield after dividing by two, using symmetry:

$$\dot{R} \iint_A \left(p_l - p_{l,\infty} - 2\,\mu_l \frac{\partial}{\partial r} v_{l,r} \right) \; \mathrm{d}S \;=\; -F_R\,\dot{R} - F_3\,U + \dot{\Phi}_{\text{halfspace}}. \tag{54}$$

The power provided at the bubble boundary, $\dot{R} \iint \left(p_l - 2\,\mu_l \frac{\partial}{\partial r} v_{l,r} \right) \; \mathrm{d}S$, is used to expel liquid at infinity, $\dot{R} \iint p_{l,\infty} \; \mathrm{d}S$, to convert, irreversibly, kinetic energy into internal energy in the space bounded by a single sphere and an infinite plane wall, $\dot{\Phi}_{\text{halfspace}}$, to move the center of mass, $-F_3\,U$, and to expand, $-F_R\,\dot{R}$. If the pressure inside the bubble is homogeneous and equal to p_b, and if viscosity effects are negligible in the bubble, the time rate of change of the kinetic energy of the bubble is zero. There is a reversible conversion of internal energy of the bubble into work at the boundary, since

$$-\iiint_{\mathcal{V}_b} p_b (\nabla\cdot\boldsymbol{v}) \; \mathrm{d}\mathcal{V} = \iint_A p_b \, \boldsymbol{v}\cdot\boldsymbol{n} \; \mathrm{d}S \;=\; p_b \frac{\mathrm{d}\mathcal{V}_b}{\mathrm{d}t}. \tag{55}$$

A similar conversion takes place in the fluid-gas interface if the area of the interface, A_b, changes, requiring the work $\sigma \, \mathrm{d}A_b/\mathrm{d}t$ where σ denotes the surface-tension coefficient. The power provided at the boundary to the liquid is therefore

$$\dot{R} \iint \left(p_l - 2\,\mu_l \frac{\partial}{\partial r} v_{l,r} \right) \; \mathrm{d}S \;=\; p_b \frac{\mathrm{d}\mathcal{V}_b}{\mathrm{d}t} - \sigma \frac{\mathrm{d}A_b}{\mathrm{d}t}. \tag{56}$$

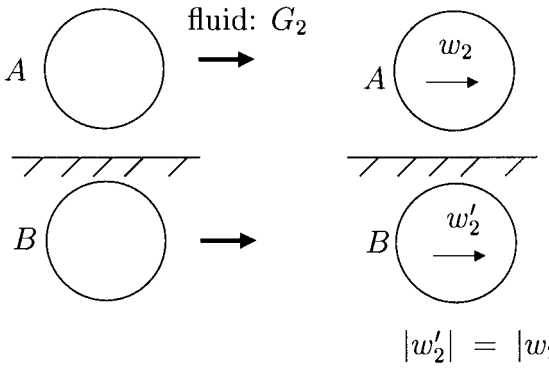

Figure 4. Definition of the two flow cases $I\,I$ and $I\,I\,I$ in the laboratory frame.

A drag force $\partial \mathcal{W}/\partial \dot{R}$ is connected to $\dot{\Phi}_{\text{halfspace}}$, as will be shown in Section 7. The $\dot{R}$-component of the power is independent of the U-component, by definition of generalized coordinates, and Equations (54) and (56) therefore yield

$$\frac{F_R}{4\,\pi\,R^2} \;=\; -p_b + p_{l,\,\infty} + \frac{2\,\sigma}{R} + \frac{1}{4\pi R^2}\frac{\partial \mathcal{W}}{\partial \dot{R}}. \tag{57}$$

Equations (57) and (50) yield the extended Rayleigh equation as a lengthy expression containing $\ddot{R}$ and $\dot{U}$. Employing the approximation (32), the leading terms in $\ddot{R}$, U, and $\dot{R}^2$ yield, see (51):

$$\begin{aligned} -\ddot{R}\,R\,(1+y) - \dot{R}^2\,\left(\tfrac{3}{2}+2\,y\right) + \tfrac{1}{2}\,\dot{U}\,R\,y^2\,h_1 + \cdots \;=\; & -\frac{p_b}{\rho_l} + \frac{p_{l,\,\infty}}{\rho_l} + \frac{2\,\sigma}{R\,\rho_l} \\ & + \frac{1}{4\pi R^2}\frac{\partial \mathcal{W}}{\partial \dot{R}} \end{aligned} \tag{58}$$

The dots on the LHS of (58) indicate terms that have been omitted for clarity and brevity. When $U = \dot{U} = y = 0$, the single-bubble case, the term $(4\pi R^2)^{-1}\partial \mathcal{W}/\partial \dot{R}$ in Section 7 will be seen to give $4\nu_l \dot{R}/R$, where $\nu_l \stackrel{\text{def}}{=} \mu_l/\rho_l$ is the kinematic viscosity. In this case (58) therefore gives the well-known Rayleigh-Plesset equation.

6. General motion

In the present section, motion of the bubble centroid in an arbitrary direction is considered. The frame of reference is the laboratory frame in which the wall is at rest in order not to invoke 'fictitious' forces.

Let the flow situation depicted in Figure 1 be named case I. With respect to the laboratory frame, arbitrary irrotational flow can be decomposed in the three cases I, $I\,I$, and $I\,I\,I$ of Figures 1 and 4. For $r < z$, the velocity potentials[3] corresponding to these flow cases are

[3]The time-dependent velocity potential coefficients $\{\tilde{e}_n,\ \tilde{k}_n\}_n$ can be transformed into coefficients $\{e_n,\ k_n\}_n$ using **E**, as discussed in Appendix A.

given by:

$$\phi_{II} = -G_2\, r\, \cos(\chi)\, P_1^1 + \sum_{n=1}^{\infty}\left[\left(\frac{r}{R}\right)^{-n-1}\tilde{e}_n + \sum_{q=1}^{\infty}\tilde{e}_q\binom{q+n}{n+1}\left(\frac{r}{z}\right)^n\left(\frac{R}{z}\right)^{q+1}\right]\cos(\chi)\, P_n^1, \tag{59a}$$

$$\phi_{III} = -\sum_{n=1}^{\infty}\tilde{k}_n\, \cos(\chi)\left\{\left(\frac{r}{R}\right)^{-n-1} P_n^1 + \sum_{q=1}^{\infty}\binom{n+q}{q+1}\left(\frac{r}{z}\right)^q\left(\frac{R}{z}\right)^{n+1} P_q^1\right\}. \tag{59b}$$

Here $(r,\ \theta,\ \chi)$ is a spherical coordinate system centered at bubble A; see Figure 1. Note that $P_o^1 = 0$. Each velocity potential can be derived by using symmetry properties of the flow situation, while converting the coordinate system $(r,\ \theta,\ \chi)$ to a $(r',\ \theta',\ \chi')$-system centered at bubble B. The boundary conditions are indicated in Figure 4, and read

$$\left.\frac{\partial\phi_{II}}{\partial r}\right|_{r=R,\,A} = 0, \qquad \left.\frac{\partial\phi_{II}}{\partial r'}\right|_{r'=R,\,B} = 0$$

$$\left.\frac{\partial\phi_{III}}{\partial r}\right|_{r=R,\,A} = w_2\, \cos(\chi)\, \sin(\theta), \quad \left.\frac{\partial\phi_{III}}{\partial r'}\right|_{r'=R,\,B} = w_2\, \cos(\chi')\, \sin(\theta').$$

Since in each flow case the same set of expansion coefficients holds for both bubbles, the following expressions (60), derived from Equation (59) and the boundary conditions, apply to both bubbles:

$$\sum_{m=1}^{\infty}\left\{-\delta_{nm} + \binom{m+n}{n+1}\frac{n}{n+1}\left(\frac{R}{z}\right)^{n+m+1}\right\}\tilde{e}_m = G_2\, \tfrac{1}{2}\, R\, \delta_{n1}, \tag{60a}$$

$$\sum_{m=1}^{\infty}\left\{-\delta_{nm} + \binom{m+n}{n+1}\frac{n}{n+1}\left(\frac{R}{z}\right)^{n+m+1}\right\}\tilde{k}_m = w_2\, \tfrac{1}{2}\, R\, \delta_{n1}. \tag{60b}$$

If the term in brackets on the LHS of Equation (60b) is named G_{nm}^{III}, the coefficients $\{\tilde{k}_m\}_m$ follow from

$$\tilde{k}_j = ([G^{III}]^{-1})_{j1}\, \tfrac{1}{2}\, R\, w_2, \tag{61}$$

while for case II the *same* operator $\mathbf{G}^{III}$ can be used:

$$\tilde{e}_j = ([G^{III}]^{-1})_{j1}\, \tfrac{1}{2}\, R\, G_2. \tag{62}$$

Case II was also studied by, for example, Miloh *et al.* [24] and Kok [17]. Case III is a straightforward extension. The special features introduced in the present paper are the deformation case I and the function $\mathbf{G}^{-1}$ to generate velocity expansion coefficients.

The velocity field around an isotropically expanding bubble in the vicinity of a plane, infinite wall is described by the potentials of the cases I, II, and III. Its motion can be

predicted using the Lagrangian approach. To this end, the kinetic-energy equation (63) is determined:

$$\frac{2\,T}{\rho_l} \;=\; \mathcal{V}_b\,\alpha_{3\,3}\,U^2 + \mathcal{V}_b\,\dot{R}^2\,\mathrm{tr}(\beta) - \mathcal{V}\dot{R}\,U\,\psi_3 + \mathcal{V}_b\,\alpha_{22}\,(w_2 - G_2)^2\,. \tag{63}$$

The added-mass coefficient α_{22} is computed in a way discussed in Section 2. It is given by

$$\alpha_{22} \;=\; -1 - \tfrac{3}{2}\,([G^{III}]^{-1})_{11}. \tag{64}$$

In the approximation of Equation (32), $\alpha_{22} \approx -1 + \frac{3}{2}\left(1 - \frac{1}{2}y^3\right)^{-1}$, see Figure 2.

Since $\dfrac{\partial \alpha_{22}\,\mathcal{V}_b}{\partial U} = 0$, the force on the center of mass in the direction x_3' is given by Equation (25) if

$$(w_2 - G_2)^2\;\mathcal{V}_b\,\frac{\partial \alpha_{22}}{\partial z} \tag{65}$$

is added to the RHS of (25) in order to account for both w_2 and G_2. The forces being known, the acceleration of the bubble, and its trajectory, can be predicted. Sample computations will be given in Section 8.

7. The drag on an expanding bubble

7.1. Viscous dissipation in potential flow

It is well known that the drag coefficient of a sphere in an unbounded fluid is given by $24/\mathrm{Re}$ in creeping flow, $48/\mathrm{Re}$ in potential flow and some value in-between if the free-surface boundary layer is taken into account. Here $\mathrm{Re} = 2\,R\,U_{\mathrm{rel}}/\nu_l$, U_{rel} being the undisturbed velocity of the liquid relative to the bubble and ν_l the kinematic viscosity of the liquid. The potential-flow approximation, applicable when $\mathrm{Re} \gg 1$, yields velocity gradients from which the rate of viscous dissipation of energy can be computed. This was first applied by Levich [30, p. 368]. The dissipation in the liquid outside an isotropically expanding sphere in the vicinity of a plane, infinite wall is now computed following the same approach. In Subsection 7.2, the result will be used to derive expressions for the drag in the Lagrangian formalism.

For a sphere, the energy dissipation rate, $\dot{\Phi}$, can be computed with

$$\dot{\Phi} \;=\; -\mu_l \iint 2\,\boldsymbol{v}\cdot \left.\frac{\partial}{\partial r}\right|_{r=R} \boldsymbol{v}\;\mathrm{d}S. \tag{66}$$

Straightforward, but tedious, calculations yield for the dissipation rate in the halfplane outside a bubble near a plane wall

$$\begin{aligned}\dot{\Phi} \;=\; & 8\,\pi\,\mu_l\,R^{-1}\sum_{n=1}^{\infty}\frac{1}{n}\,(2\,n+1)\,(n+1)\,\tilde{a}_{n+1}^2 + 16\,\pi\,\mu_l\,R\,\dot{R}^2 + \\ & +4\,\pi\,\mu_l\,R^{-1}\sum_{n=1}^{\infty}(2\,n+1)\,(n+1)^2\,(\tilde{k}_n - \tilde{e}_n)^2.\end{aligned} \tag{67}$$

In this computation of $\dot{\Phi}$, use has been made of Equation (68) which has not been found in the literature:

$$\int_{-1}^{1} \mathrm{d}x\ (1-x^2)\,\frac{\mathrm{d}P_q^1}{\mathrm{d}x}\,\frac{\mathrm{d}P_n^1}{\mathrm{d}x} \;=\; \begin{cases} q\,(q+1)\,(2\,q^2-1)/(2\,q+1) & \text{if } n=q \\ -\frac{1}{2}\,\{1+(-1)^{n-q}\}\,(q+1)\,q & \text{if } q\le n-2 \end{cases}. \tag{68}$$

Kok [16, Chapter 3] performed a similar computation for the case of two rigid spheres, and derived Equation (67) without the $R\,\dot{R}^2$-term and with a different meaning of the coefficients $\{\tilde{a}_n\}$. Equation (67) is used in Section 7.2 to compute the drag on the bubble.

7.2. Drag in the Lagrangian formalism

Moore [32] took the free-surface boundary layer into account, and showed that the dissipation of a freely rising bubble yields a drag coefficient that is given by

$$c_D \;=\; \frac{48}{\mathrm{Re}} - \frac{106}{\mathrm{Re}^{3/2}}. \tag{69}$$

This shows that the drag of non-deforming spheres can be overestimated to within an accuracy of $\mathrm{Re}^{-3/2}$ by considering potential flow only. In the case of a fast growing bubble the free-surface boundary layer may not be well-developed, and the potential-flow approximation is even more accurate. It will now be seen how the Lagrangian formalism can account for a $(\mathrm{Re}\to c_D)$–relationship like that of Equation (69).

Suppose that a function $\mathcal{W}$ exists such that

$$\dot{\Phi} \;=\; \sum_{j=1}^{N} \dot{q}^j\,\frac{\partial \mathcal{W}}{\partial \dot{q}^j}; \tag{70}$$

then each $\left(-\,\partial\mathcal{W}/\partial\dot{q}^i\right)$ represents a drag force on the fluid. This drag force will be denoted by $Q_{\mathcal{W},i}$. Two important examples of $\mathcal{W}$ are now considered. Suppose that Φ is given by $\dot{\Phi} \;=\; W_{ij}\,\dot{q}_i\,\dot{q}_j$ for $\dot{q}_i$-independent functions W_{ij}. Then $\mathcal{W} = \frac{1}{2}\,\dot{\Phi}$ and $\mathcal{W}$ is called Rayleigh's dissipation function. If, alternatively, Φ is given by

$$\dot{\Phi} \;=\; W_1\,\dot{q}_1^2 - W_2\,\dot{q}_1^{3/2},$$

then

$$\mathcal{W} \;=\; \tfrac{1}{2}\,W_1\,\dot{q}_1^2 - \frac{2}{3}\,W_2\,\dot{q}_1^{3/2}$$

and $Q_{\mathcal{W},1} \;=\; -W_1\,\dot{q}_1 + W_2\,\dot{q}_1^{1/2}$ represents the drag force with c_D given by Equation (69). This shows that the dissipation function $\mathcal{W}$ offers a generalisation of Rayleigh's dissipation function that may accommodate the boundary-layer dissipation at free-surfaces to an accuracy of $\mathrm{Re}^{-3/2}$. Higher accuracies are obtained, naturally, by considering $\mathcal{W} \;=\; \sum_{j=1}^{N} f_j\,\dot{q}^{n_j}$ with exponents n_j and coefficients f_j fitted to more accurate expressions of $\dot{\Phi}$.

The hydrodynamic forces computed in the previous sections and the drag force $Q_{\mathcal{W},i}$ jointly determine the bubble trajectory. Consider, as an example, the case that $\dot{R}(t)$ is prescribed for a spherically growing or collapsing bubble in motion perpendicular to the wall.

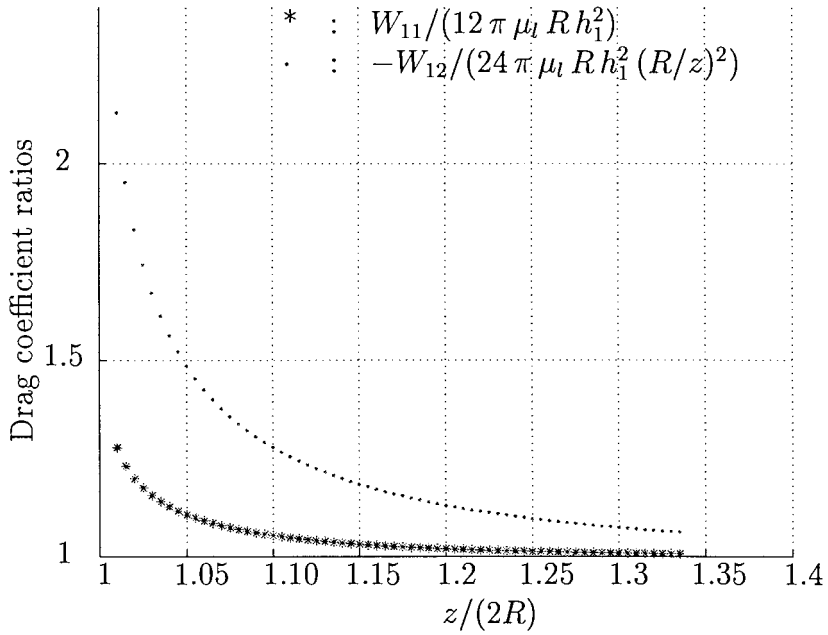

Figure 5. Ratios of drag force coefficients to approximations in the vicinity of the wall.

Since the $\dot{R}$-history is prescribed, the extended Rayleigh equation does not have to be solved. With the aid of Equation (67), Rayleigh's dissipation function is found to be given by

$$W_{11} \;=\; 2\,\pi\,\mu\,R\sum_{n=1}^{\infty}\frac{1}{n}\,(2\,n+1)\,(n+1)\,(G^{-1}_{(n+1)\,2})^2, \tag{71a}$$

$$W_{12} \;=\; W_{21} \;=\; -8\,\pi\,\mu\,R\sum_{n=1}^{\infty}\frac{1}{n}\,(2\,n+1)\,(n+1)\,G^{-1}_{(n+1)\,1}\,G^{-1}_{(n+1)\,2}. \tag{71b}$$

The component of the friction force in direction $\mathbf{e}_3$ on the bubble is given by $\partial\left(\frac{1}{2}\dot{\Phi}\right)/\partial U$. This expression yields the following balance of hydrodynamic and drag forces in direction $\mathbf{e}_3$:

$$\alpha_{33}\,\dot{U}\,\mathcal{V}_b \;-\; \tfrac{1}{2}\,\psi_3\,\ddot{R}\,\mathcal{V}_b + U\,\dot{R}\left\{\mathcal{V}_b\,\frac{\partial\alpha_{33}}{\partial R} + 4\,\pi\,R^2\,\alpha_{33}\right\} + U^2\,\mathcal{V}_b\,\frac{\partial\alpha_{33}}{\partial z} + \tfrac{1}{2}\,\dot{R}^2\left\{\mathcal{V}_b\,\frac{\partial\psi_3}{\partial R}\right.$$
$$\left. + 2\,\mathcal{V}_b\,\frac{\partial \mathrm{tr}(\beta)}{\partial z} + 4\,\pi\,R^2\,\psi_3\right\} \;=\; \left(-W_{11}\,U - W_{12}\,\dot{R}\right)/\rho_l. \tag{72a}$$

The displacement of the centroid follows from

$$\dot{z} \;=\; 2U. \tag{72b}$$

Equation (72) can be integrated numerically in time to solve for U and z. In this way the trajectory of the bubble can be determined for any set of initial values of z, R, U, and for any given history of the radius, $\dot{R}(t)$. If only the initial value of $\dot{R}$ is specified, (72) has to be solved jointly with the extended Rayleigh equation.

In many cases, the predictions can be improved by incorporating a term $-\tilde{W}_{11}\,U^{1/2}$, as explained above. At large distances from the wall, *i.e.*, if $y \ll 1$, $\tilde{W}_{11}/W_{11} \sim 106/48$, see(69).

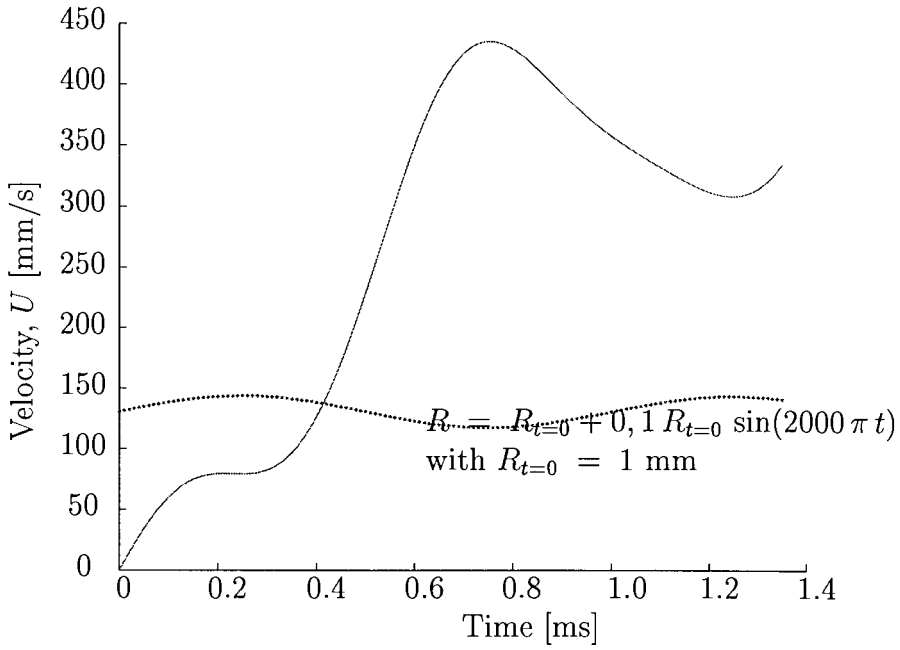

Figure 6. History of velocity U for a bubble with an oscillating radius, starting from rest ($U = 0$). The corresponding imposed radius history is indicated as a dotted line.

In the approximation of Equation (32), Equation (71) yields

$$W_{11} \sim 12\,\pi\,\mu\, R\, h_1^2 \quad \text{and} \quad W_{12} \sim -24\,\pi\,\mu\, h_1^2\, R\,(R/z)^2 = -2\, W_{11}\,(R/z)^2. \tag{73}$$

An expanding bubble therefore experiences *less* drag then an imploding bubble in motion away from the wall ($U > 0$). Figure 5 shows that the W_{11} given by Equation (73) is accurate to $\pm 5\%$ if $(\frac{1}{2}z/R) > 1{\cdot}2$. For $h_1 \sim 1$, *i.e.*, for a sphere in an unbounded fluid, Equation (73) yields the well-known drag coefficient $c_D = 48/\mathrm{Re}$.

8. Sample trajectory computations

Interest in the hydrodynamic interaction of two oscillating bubbles has a long history that goes back to Bjerknes; see Section 1. The first example of the present section deals with the nonlinear interaction of two oscillating bubbles, one being the mirror bubble B of Figure 1.

If the hydrodynamic forces do not affect the shapes of the bubbles, the two governing equations to be solved are given by (72). Using (71) and the right-hand side of (49), this has been done for the initial conditions $U(t = 0) = 0$ mm/s, $R(t = 0) = R_{t=0} = 1$ mm, initial distance of the two centres $2{\cdot}24\, R_{t=0}$ and for a prescribed shape history corresponding to an oscillating bubble:

$$R = R_{t=0} + 0{\cdot}1\, R_{t=0}\, \sin(2000\,\pi\, t).$$

The period of oscillation, T, has been chosen small as compared to the characteristic time corresponding to the drag force, $R_{t=0}^2\, \rho_l/(18\,\mu_l)$, with $\rho_l = 1000$ kg/m^3, $\mu_l = 10^{-3}$ m^2/s. The corresponding frequency is that of the periodic part of a solution of the Rayleigh equation [5,

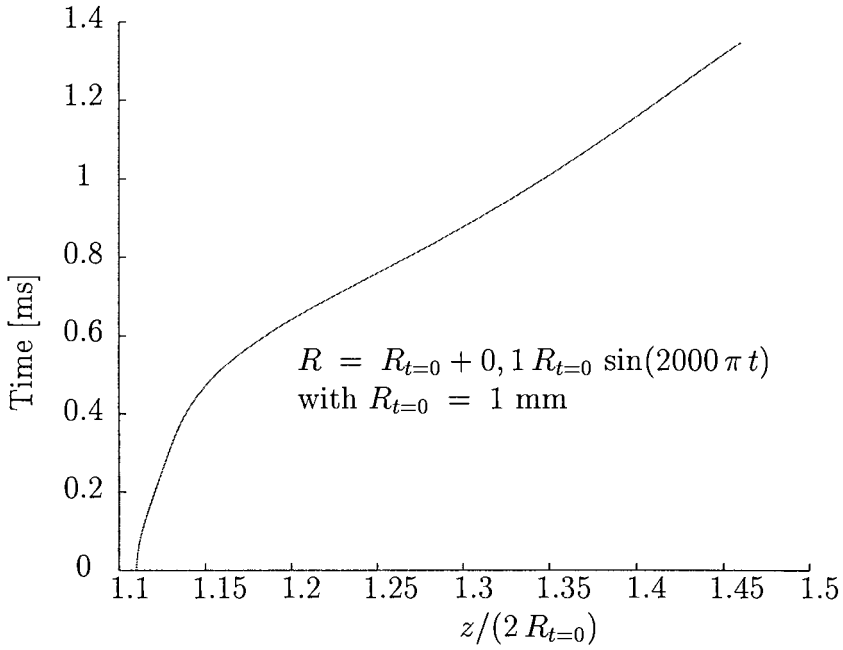

Figure 7. Trajectory of a bubble with an oscillating radius in the vicinity of a plane, infinite wall. See Figure 6.

p. 101]:

$$\frac{2\,\pi}{T} = \left\{ \frac{3\, p_{l,\infty}\, \gamma}{\rho_l\, R_{t=0}^2} + \frac{2\,\sigma(3\,\gamma - 1)}{\rho_l\, R_{t=0}^3} \right\}^{-0.5},$$

if the pressure at infinity, $p_{l,\infty}$, is suitably chosen. Here $\gamma \stackrel{\text{def}}{=} c_p/c_v$. The change in velocity during the first $1\frac{1}{2}$ period of oscillation is shown in Figure 6, the corresponding trajectory in Figure 7 and the force history in Figure 8. the bubble propels itself away from the wall[4]. This self-propulsion of a homogeneous sphere is induced by the mirror sphere (or the wall), since Saffman [29] showed that in the absence of a wall a homogeneous body requires asymmetrical deformations in order to experience a persistent motion of its centroid. The computed force has a sign opposite to what would be expected on the basis of the linear theory for the Bjerknes forces [10], which is due to nonlinearity and the fact that the oscillation is not free to satisfy the extended Rayleigh equation (50) exactly.

Another important example is that of a boiling bubble at the verge of detachment from a vertical plane wall when gravity plays an insignificant role [2]. Expressions for the forces acting on the bubble are often modified to predict the detachment radius [33]. In many cases, depending on pressure and heat flux, the shape just before detachment is close to spherical, the growth rate is controlled by diffusion and proportional to $t^{1/2}$, and the bubble foot negligibly small [34]. With forced convection, the velocity G_2 of the liquid at infinity depends on the distance of the bubble center from the wall, $z/2$. These ingredients are used in the following

[4]Submarines might use this principle to leave dock without making a sound, *e.g.*, by inflating a large part of a flexible belly at high frequency. Surface waves might probably not be avoided, however.

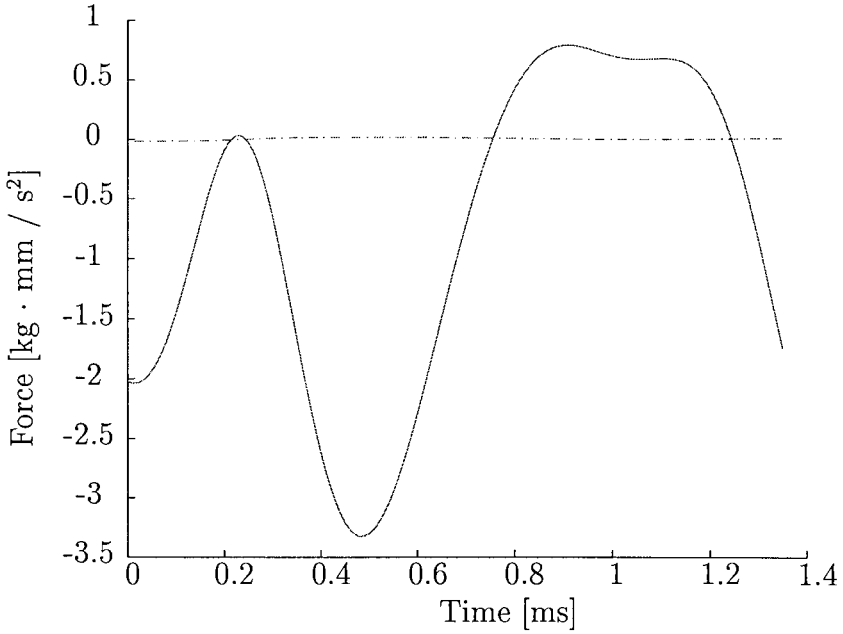

Figure 8. Histories of forces on bubble in the vicinity of a plane wall. The dotted line is the drag force and the solid line the hydrodynamic minus the terms proportional to $\ddot{R}$ and $\dot{U}$.

example:

$$R_{t=0} = 0{\cdot}2 \text{ mm} \quad \text{and} \quad U_{t=0} = 1{\cdot}32 \text{ mm/s} \quad \text{and} \quad z_{t=0} = 4{\cdot}4\, R_{t=0},$$
$$t_o = 0{\cdot}005\, R_{t=0}^2 \text{ s} \quad \text{and} \quad R = \frac{1}{\sqrt{0{\cdot}005}} \sqrt{t + t_o} \text{ mm},$$
$$G_2 = -50\, z \text{ mm/s} \quad \text{and} \quad w_2 = 0.$$

The remaining parameters are the same as in the previous example. Expression (65) is added to the LHS of (72a). The results (Figures 9 and 10) show that the force corresponding to G_2^2 presses the bubble to the wall and is quite significant. Figure 10 shows that the hydrodynamic lift [35]

$$F_{\text{lift},\, x_3'} = -2\mathcal{V}_b\, \rho_l\, c_L\, \frac{\partial G_2}{\partial z}\, (w_2 - G_2) = -\mathcal{V}_b\, \rho_l\, 100^2\, z\, c_L/2 \tag{74}$$

is smaller than the counteracting hydrodynamic force corresponding to G_2^2 by about a factor four. The lift force pushes the bubble away from the wall. The lift-force coefficient, c_L, is taken to be 0·5 despite the fact that it is known to depend on the added-mass coefficients and on Re [36]. A detailed discussion of the lift force is beyond the scope of the present investigation, and the lift force has therefore not been included in the equation of motion of the bubble centroid.

9. Conclusions

Equations for the acceleration and spherical deformation of a bubble in a potential flow in the vicinity of a plane infinite wall have been derived. A solution method for the velocity

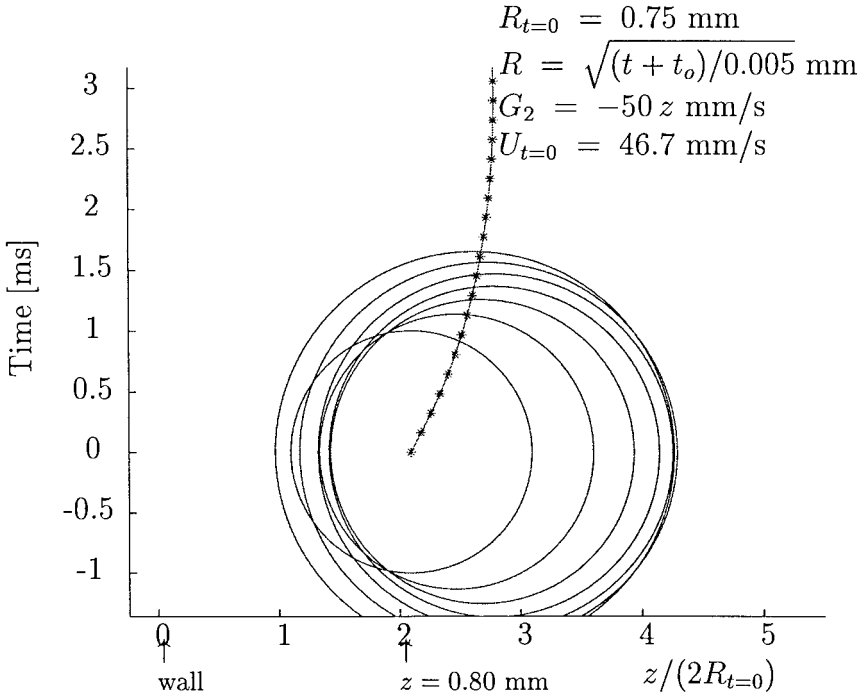

Figure 9. Trajectory and shape history of a bubble growing in the vicinity of a plane wall. The shape is prescribed and not shown at each instant of time.

potential, ϕ, has been introduced that is based on an operator on $l^2(\phi)$. This solution method can also be applied to arbitrary deformation of the bubble.

The Lagrange–Thomson approach to compute hydrodynamic forces has been applied. The acceleration of the bubble center was shown to be equal to the acceleration predicted with the Lagally theorem. It is shown that deformation monopoles do not contribute to the $\mathrm{d}/\mathrm{d}t$-term of the Lagally theorem, the so-called acceleration reaction. Some mistakes made by previous authors were discovered and have been rectified. The Levich approach has been applied to take viscous dissipation into account. The Rayleigh dissipation function has been extended to account for the free-surface boundary layer. The drag force on an expanding spherical bubble in arbitrary motion in the vicinity of a plane wall has been computed. It depends on U, $\dot{R}$ and the distance to the wall. Asymptotic solutions of hydrodynamic and drag forces are in good agreement with results of the literature.

An extended Rayleigh–Plesset equation has been derived that describes deformation in the vicinity of a plane wall. Asymptotic solutions are in agreement with previous results.

Two sample shape histories and trajectories were computed with truncations for which it is possible to estimate the residual error. These examples correspond to practical engineering problems in which capillary forces dominate inertial forces.

Future studies will be devoted to the application of the results of the present study to the derivation of criteria for bubble detachment [33] and to the modeling of an arbitrarily deforming bubble near a solid wall [37].

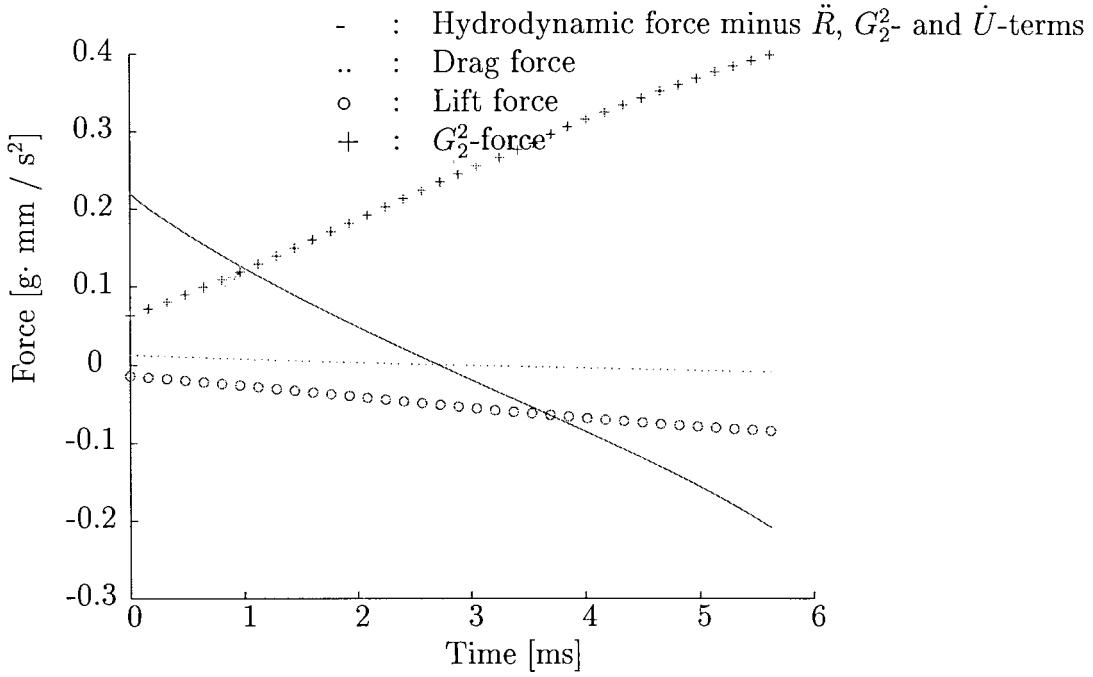

Figure 10. Force histories corresponding to Figure 9, see caption Figure 9.

Acknowledgements

The author thanks Dr W.W.F. Pijnappel for his help in deriving the symmetry of $\mathbf{B} \cdot \mathbf{D}^{-1}$, see Appendix 9, Dr J.G.M. Kuerten for carefully reading the manuscript, and Professor C. Pozrikidis for many valuable suggestions to improve the presentation.

Appendix A. Convergence and the operator G

It can be shown that

$$\sum_{i,j=1}^{\infty} |\alpha_{ij}|^2 = \sum_{i=1}^{\infty} b_i \stackrel{\text{def}}{=}$$

$$\stackrel{\text{def}}{=} \sum_{i=1}^{\infty} \left(\frac{i-1}{i}\right)^2 R^{4i-2} z^{-2i} \left(1-z^{-2}\right)^{-2i+1} \sum_{j=1}^{i-1} \binom{i-1}{j}^2 z^{-2j},$$

which converges if $z > 1$ and if $\lim_{i\to\infty} b_{i+1}/b_i = R^4 z^{-2} \left(1-z^{-2}\right)^2 \left(\frac{z+1}{z}\right)^2 < 1$. This is satisfied if

$$z > 1 \qquad \text{and} \qquad R < \sqrt{z-1}. \tag{A1}$$

From Equation (A1) the condition $R/z < \frac{1}{2}$ is easily recovered. In practical computations, Equation (A1) can be satisfied by adaptation of the unit length. Alternatively, the operator **G** is used defined by

$$G_{ij} \stackrel{\text{def}}{=} -\delta_{ij} + \frac{i-1}{i} \left(\frac{R}{z}\right)^{i+j-1} \binom{i+j-2}{i-1}. \tag{A2}$$

The boundary condition (2) now takes the form

$$\sum_{j=1}^{\infty} G_{i\,j}\,\tilde{a}_j \;=\; R\,\dot{R}\,\delta_{i1} - \tfrac{1}{2}\,R\,U\,\delta_{i2}. \tag{A3}$$

The operator $\mathbf{G}^{-1}$ exists if either $\dot{R} \neq 0$ or $U \neq 0$. It is therefore easier to apply operator $\mathbf{G}$ than it is to apply operator $\mathbf{F}$.

The connection between $\mathbf{F}$ and $\mathbf{G}$ is given by the scaling operator $\mathbf{E}$ defined by

$$E_{i\,j} \;\stackrel{\text{def}}{=}\; R^{-i}\,\delta_{i\,j}. \tag{A4}$$

For $a \in l^2(\phi)$, $\tilde{a} \stackrel{\text{def}}{=} \mathbf{E}\,a$, $\mathbf{F} = \mathbf{E}^{-1}\,\mathbf{G}\,\mathbf{E}$, $\mathbf{F}^{-1} = \mathbf{E}^{-1}\,\mathbf{G}^{-1}\,\mathbf{E}$. Then $F_{ij}^{-1} = R^{i-j}\,G_{ij}^{-1}$. However, only if $\mathbf{F}$ exists, *i.e.*, if Equation (A1) is satisfied, $\mathbf{E}$ can be used to map $\mathbf{F}$ to $\mathbf{G}$, but, in general, $\mathbf{E}$ is not an isometrical operator, since the dual $\mathbf{E}^*$ equals $\mathbf{E}$ and $\mathbf{E}^* \cdot \mathbf{E} \neq \mathbf{I}$.

Appendix B. Proof of a symmetry relation

To prove Equation (8), we first note that $F_{11} = -1$, and $F_{1j} = 0$ if $j > 1$, while F_{i1} is nonzero if $i > 1$. Define

$$\tilde{b} \stackrel{\text{def}}{=} (F_{21}^{-1},\; F_{31}^{-1},\; F_{41}^{-1}, \dots)^T, \tag{B1a}$$

$$\tilde{c} \stackrel{\text{def}}{=} (F_{21},\; F_{31},\; F_{41}, \dots)^T, \tag{B1b}$$

$$B_{i\,j} \stackrel{\text{def}}{=} F_{i+1\;j+1}^{-1}, \qquad i, j \in I\!N\backslash\{0\}, \tag{B1c}$$

$$C_{i\,j} \stackrel{\text{def}}{=} F_{i+1\;j+1} + \delta_{i\,j}, \qquad i, j \in I\!N\backslash\{0\}. \tag{B1d}$$

The functions $\mathbf{F}$ and $\mathbf{F}^{-1}$ now take the form

$$\underline{\underline{F}} \;=\; \begin{pmatrix} -1 & \underline{0} \\ \tilde{c} & \underline{\underline{C}} - \underline{\underline{I}} \end{pmatrix}, \qquad \underline{\underline{F}}^{-1} \;=\; \begin{pmatrix} -1 & \underline{0} \\ \tilde{b} & \underline{\underline{B}} \end{pmatrix}, \tag{B2}$$

where $\underline{0}$ denotes the row-vector with only zeroes. The equation $\mathbf{F}\cdot\mathbf{F}^{-1} = \mathbf{I}$ yields $(\mathbf{C} - \mathbf{I})\cdot\mathbf{B} = \mathbf{I}$ and $-\tilde{c} + (\mathbf{C} - \mathbf{I}) \cdot \tilde{b} = 0$, whence

$$\tilde{b} \;=\; (\mathbf{C} - \mathbf{I})^{-1}\,\tilde{c} \;=\; \mathbf{B}\,\tilde{c} \tag{B3}$$

The diagonal function $\mathbf{D}$ is defined by

$$D_{i\,j} \;=\; \frac{i+1}{i}\,R^{-1-2i}\,\delta_{i\,j}. \tag{B4}$$

Since

$$(D \cdot C)_{i\,j} \;=\; z^{-1-i-j}\,(i+j)!\;\{i!\;j!\}^{-1}, \tag{B5}$$

the functions $\mathbf{D}\cdot\mathbf{C}$, $\mathbf{D}\cdot(\mathbf{C}-\mathbf{I})$ and its inverse $(\mathbf{D}\cdot(\mathbf{C}-\mathbf{I}))^{-1}$ are symmetric. Since (B3) yields

$$\mathbf{D}\cdot(\mathbf{C}-\mathbf{I})\cdot\mathbf{B}\cdot\mathbf{D}^{-1} \;=\; \mathbf{D}\cdot\mathbf{D}^{-1} \;=\; \mathbf{I},$$

$(\mathbf{D}\cdot\mathbf{C})^{-1}$ equals $\mathbf{B}\cdot\mathbf{D}^{-1}$. Equation (8) merely expresses the fact that $\mathbf{B}\cdot\mathbf{D}^{-1}$ is symmetric.

Equation (B3) gives $F^{-1}_{(i+1)\,1} = \tilde{b}_i = B_{ij}\,\tilde{c}_j$. So

$$F^{-1}_{(i+1)\,1} = \sum_{j=1}^{\infty} F^{-1}_{(i+1)\;(j+1)}\,F_{(j+1)\,1} = \sum_{j=1}^{\infty} F^{-1}_{(i+1)\;(j+1)}\,\frac{j}{j+1}\,R^{2j+1}\,z^{-j-1}.$$

If Equation (8) is used to switch the indices, Equation (9) is obtained.

Appendix C. Derivation of Equations (42) and (43)

The Leibniz theorem in its general form reads

$$\frac{\mathrm{d}}{\mathrm{d}t}\iiint f\;\mathrm{d}\mathcal{V} = \iiint \frac{\partial f}{\partial t}\,\mathrm{d}\mathcal{V} + \iint f\;\vec{u}\cdot\boldsymbol{n}\;\mathrm{d}S \tag{C1}$$

for any function $f \;\in\; C^{\infty}$. The volume of integration is $\mathcal{V}_b$. Take f to be an arbitrary coordinate function, x_i, to find

$$\iint x_i\;\boldsymbol{u}\cdot\boldsymbol{n}\,\mathrm{d}S = \frac{\mathrm{d}}{\mathrm{d}t}\iiint x_i\,\mathrm{d}\mathcal{V} - \iiint \frac{\partial x_i}{\partial t}\,\mathrm{d}\mathcal{V} = \frac{\mathrm{d}}{\mathrm{d}t}\iiint x_i\,\mathrm{d}\mathcal{V} = \frac{\mathrm{d}}{\mathrm{d}t}\left(x_{c,i}\,\mathcal{V}_b\right) \tag{C2}$$

Using (41) and (C2), we find Equation (42). Using the divergence theorem, we find

$$\iint x_i\,n_j\;\mathrm{d}S \;=\; \delta_{ij}\,\mathcal{V}_b. \tag{C3}$$

The other integral of (42) yields

$$\boldsymbol{x}_c\iint \boldsymbol{v}_d\cdot\boldsymbol{n}\;\mathrm{d}^2x + \iint x_i'\,\boldsymbol{v}_d\cdot\boldsymbol{n}\;\mathrm{d}S. \tag{C4}$$

Taking $f = 1$ in (C1) we obtain

$$\frac{\mathrm{d}}{\mathrm{d}t}\mathcal{V}_b \;=\; \boldsymbol{v}_c\cdot\iint\boldsymbol{n}\;\mathrm{d}S + \iint\boldsymbol{v}_d\cdot\boldsymbol{n}\;\mathrm{d}S,$$

which can be combined with

$$\iint\boldsymbol{n}\;\mathrm{d}^2x \;=\; 0 \tag{C5}$$

to give

$$\iint\boldsymbol{v}_d\cdot\boldsymbol{n}\;\mathrm{d}S \;=\; \frac{\mathrm{d}}{\mathrm{d}t}\mathcal{V}_b. \tag{C6}$$

We now combine (42), (C3), (C4), and (C6) to obtain

$$\frac{\mathrm{d}}{\mathrm{d}t}\left(x_{c,i}\,\mathcal{V}_b\right) \;=\; v_{c,i}\,\mathcal{V}_b + x_{c,i}\,\frac{\mathrm{d}\mathcal{V}_b}{\mathrm{d}t} + \iint x_i'\,\boldsymbol{v}_d\cdot\boldsymbol{n}\;\mathrm{d}S. \tag{C7}$$

The chain rule gives

$$\frac{\mathrm{d}}{\mathrm{d}t}\,(x_{c,i}\,\mathcal{V}_b) \;=\; v_{c,i}\,\mathcal{V}_b + x_{c,i}\,\frac{\mathrm{d}\mathcal{V}_b}{\mathrm{d}t}.$$

Equation (C7) therefore yields Equation (43).

References

1. J. F. Klausner, R. Mei, D. M. Bernard and L. Z. Zeng, Vapor bubble departure in forced convection boiling. *Int. J. Heat Mass Transfer* 36 (1993) 651–661.
2. W. G. J. van Helden, C. W. M. van der Geld and P. G. M. Boot, Forces on bubbles growing and detaching in flow along a vertical wall. *Int. J. Heat Mass Transfer* 38 (1995) 2075–2088.
3. H. Yuan and A. Prosperetti, Gas-liquid heat transfer in a bubble collapsing near a wall. *Phys. Fluids* 9 (1997) 127–142.
4. N. A. Pelekasis and J. A. Tsamopoulos, Bjerknes forces between two bubbles. part 1. response to a step change in pressure. *J. Fluid Mech.* 254 (1993) 467–499.
5. C. E. Brennen, *Cavitation and Bubble Dynamics*. Oxford: Oxford University Press (1995) 282 pp.
6. S. van Stralen and R. Cole, *Boiling Phenomena*, Volume 1 and 2. Washington: McGraw-Hill (1979) 457 pp. and 498 pp.
7. R. E. Apfel, Technique for measuring the adiabatic compressibility, density and sound speed of sub-microliter liquid samples. *J. Acoust. Soc. Am.* 59 (1976) 339–343.
8. M. A. H. Weiser, R. E. Apfel and E. A. Neppiras, Interparticle forces on red cells in a standing wave field. *Acustica* 56 (1984) 114–119.
9. A. Prosperetti, Bubble phenomena in sound fields: part two. *Ultrasonics* 22 (1984) 115–123.
10. H. N. Oguz and A. Prosperetti, A generalization of the impulse and virial theorems with an application to bubble oscillations. *J. Fluid Mech.* 218 (1990) 143–162.
11. T. Brooke Benjamin, Hamiltonian theory for motions of bubbles in an infinite liquid. *J. Fluid Mech.* 181 (1987) 349–379.
12. A. Galper and T. Miloh, Dynamic equations of motion for a rigid or deformable body in an arbitrary non-uniform potential flow field. *J. Fluid Mech.* 295 (1995) 91–120.
13. Y. Yurkovetsky and J. F. Brady, Statistical mechanics of bubbly liquids. *Phys. Fluids* 8 (1996) 881–895.
14. H. Lamb, *Hydrodynamics*. (6th edition) Cambridge: Cambridge University Press (1957) 738 pp.
15. W. A. H. J. Hermans, *On the Instability of a Translating Gas Bubble Under the Influence of a Pressure Step*. Ph.D. thesis, Einhoven Univ. of Techn., (1973) pp. 107.
16. J. B. W. Kok, Dynamics of Gas Bubbles Moving Through Liquid. Ph.D. thesis, T.U. Twente (1989) pp. 116.
17. J. B. W. Kok, Dynamics of a pair of gas bubbles moving through liquid. I Theory. *Eur. J. Mech. B/Fluids* 4 (1993) 515–540.
18. P. G. Saffman, On the rise of small bubbles in water. *J. Fluid Mech.* 1 (1956) 249–275.
19. D. W. Moore, The velocity of rise of distorted gas bubbles in a liquid of small viscosity. *J. Fluid Mech.* 23 (1965) 749–766.
20. E. W. Hobson, *The Theory of Spherical and Ellipsoidal Harmonics*. Cambridge: Cambridge University Press (1955) 500 pp.
21. L. W. Kantorowich and W.I. Krylow, *Approximate Methods of Higher Analysis*. New York: Interscience Publishers (1958) 611 pp.
22. O. V. Voinov, On the motion of two spheres in a perfect fluid. *PPM* 33 (1969) 638–646.
23. C. P. Witze, V. E. Schrock and P. L. Chambré, Flow about a growing sphere in contact with a plane surface. *Int. J. Heat Mass Transfer* 11 (1968) 1637–1652.
24. T. Miloh, Hydrodynamics of deformable contiguous shapes in an incompressible inviscid fluid. *J. Eng. Math.* 11 (1977) 349–372.
25. L. Landweber and C. S. Yih, Forces, moments, and added masses for Rankine bodies. *J. Fluid Mech.* 1 (1956) 319–336.
26. L. Landweber and T. Miloh, Unsteady Lagally theorem for multipoles and deformable bodies. *J. Fluid Mech.* 96 (1980) 33–46. With Corrigendum in *J. Fluid Mech.* 112 (1981) p. 502.
27. L. v. Wijngaarden, On the motion of gas bubbles in a perfect fluid. *Arch. Mech.* 34 (1982) 343–349.

28. A. Biesheuvel, A note on the generalized Lagally theorem. *J. Eng. Math.* 19 (1985) 69–77.
29. P. G. Saffman, The self-propulsion of a deformable body in a perfect fluid. *J. Fluid Mech.* 28 (1966) 385–389.
30. G. K. Batchelor, *An Introduction to Fluid Dynamics*. Cambridge: Cambridge University Press (1967) 615 pp.
31. R. Bird, W. E. Steward and E. N. Lightfoot, *Transport Phenomena*. New York: John Wiley & Sons (1960) 780 pp.
32. D. W. Moore, The boundary layer on a spherical gas bubble. *J. Fluid Mech.* 16 (1963) 161–176.
33. C. W. M. van der Geld, A note on the bubble growth force. *Multiphase Sci. and Techn.* (2001) In the press.
34. D. Qiu and C. W. M. van der Geld, Bubble shapes and forces at detachment. In: F. Mayinger and M. Lehner (eds), *Convective Flow and Pool Boiling* London: EC4A 3DE. Eng. Foundation, Taylor & Francis (1999) pp. 271–278.
35. T. R. Auton, J. C. R. Hunt and Prud'Homme, The force exerted on a body in inviscid, unsteady non-uniform rotational flow. *J. Fluid Mech.* 197 (1988) pp. 241–257.
36. C. W. M. van der Geld, Measurement and prediction of solid sphere trajectories in accelerated gas flow. *Int. J. Multiphase Flow* 23 (1997) pp. 357–376.
37. C. W. M. van der Geld and J. G. M. Kuerten, Deformation and motion of a bubble near a plane wall. In: S. Michaelides (ed.), *Fourth Int. Conf. on Multiphase Flow* (2001) pp. 1–12.